Regular Article

Faustyn Recha*

Estimation method of corrosion current density of RC elements

https://doi.org/10.1515/eng-2022-0430
received January 07, 2023; accepted March 16, 2023

Abstract: The work is theoretical with the use of analytical calculations, subsequently confirmed by a numerical method, in which an attempt was made to verify the method of estimating the corrosion current density based on the deflection of reinforced concrete (RC) elements affected by reinforcement corrosion. The focus was on the possibility of estimating the corrosion current intensity on the basis of external measurements of deflections of RC elements subjected to reinforcement corrosion. The method can be used as an element supporting the diagnosis of RC structures. The article presents an example of analytical and numerical deflection calculations, on the basis of which an attempt was made to estimate the corrosion current density. The obtained results were considered satisfactory, which is sent for further considerations, and above all for experimental verification of the proposed method. The analysis was based on the theoretical work of a simply supported beam, whose analytical results were verified using the finite element method. For the purposes of theoretical considerations, the impact of corrosion of the beam reinforcement was assumed in the form of a history of changes in the intensity of the corrosion current obtained in another research work. Finally, the obtained results confirmed the assumptions regarding the possibility of estimating the corrosion current density on the basis of the deflection of the analyzed beam.

Keywords: corrosion of steel in reinforced concrete, deflection, corrosion rate, numerical analysis

*** Corresponding author: Faustyn Recha,** Faculty of Architecture, Civil Construction and Applied Arts, Academy of Silesia, Rolna Street 43, Katowice, Poland, e-mail: faustyn.recha@wst.pl

1 Introduction

Corrosion of reinforcing steel in reinforced concrete (RC) elements is a problem undertaken by a wide group of researchers. In the area of corrosion phenomena, two basic stages can be distinguished. The first consists in initiating the process [1,2], which concerns the coupled processes of transporting moisture, heat, and aggressive substances to the concrete cover [3–7]. After exceeding the contractual limit, a corrosion center occurs as a result of the development of electrode processes on the surface of the reinforcement, which is considered the second stage of the process consisting in the propagation of structural damage. In addition to the degradation of the cover as a result of the increase in corrosion products, taking into account various forms of void filling [8–11], there are also changes in the yield point of the reinforcing steel [12,13] or changes in the adhesion forces at the steel–concrete interface [14–17]. Ultimately, corrosion processes lead to a reduction in the load capacity of the structure [18–22]. Corrosion of reinforcing steel in RC is therefore a complex problem of durability, the analysis and development of which is fully justified by the safety of the structure operation, the possibility of using the facility, or economic aspects [23–25]. In addition to advanced diagnostic methods of RC structures [26–28], visible signs of reinforcement degradation are, among others, corrosion products carried out through the gap of the emerging crack [29], deflections of the element caused by the loss of reinforcement mass and changes in Young's modulus of steel [20,30], and structural cracks [31] arising under the influence of the progressing corrosion process.

In the article, a guess was made regarding the numerical verification of the method of estimating the corrosion current density on the basis of monitoring the deflection of a RC element presented by Recha [32], which may be the starting point for advanced diagnostics of RC structures known from the literature on the subject. In previous studies, the corrosive environment was simulated using various methods of accelerating the corrosion of reinforcement [30,33–37] or the problem was analyzed based on the

results of long-term tests of elements in conditions of real environmental aggression [20,38]. On this basis, the influence of the progressing corrosion process in various areas of consideration was presented. Currently, the article focuses on the opposite approach. An attempt was made to verify the model numerically by deriving a relationship describing the corrosion current density on the basis of the deflection curvature of an RC element [32], using the example of a specific structural element. The deflection analysis was carried out using the analytical and numerical method using the finite element method (FEM) of an exemplary RC beam. Reinforcement mass loss was assumed on the basis of the results of current measurements in the electrode cell, which were a simulation of the corrosion process carried out as part of the work [10]. On this basis, in accordance with the algorithm contained in the standard [39], the history of changes in the beam deflection was determined as a function of the duration of the accelerated corrosion test of the reinforcement, on the basis of which the correctness of the adopted method of estimating the corrosion current density was determined. Changes in the Young's modulus of reinforcement and the influence of concrete creep were not taken into account in the work. The performed calculations concern only the loss of reinforcement mass. The work is a preliminary theoretical approach, the results of which should be verified at the stage of planning further experimental research and extending by research on changes in Young's modulus and taking into account the creep of concrete. The proposed method is intended to approximate the corrosion current intensity.

2 Deflections of RC elements

Deflections of RC elements should be considered in two phases conditioned by the cracking condition of the structure [39]. Deflections of the element in the non-scratched state include the so-called Stage I of the structure's operation, in which the tensile stresses occurring in the structure do not exceed the limit values equal to the average tensile strength of the concrete f_{ctm}. Phase II occurs when the permissible tensile stress level is exceeded. The element in this situation is scratched. The scratching stage, according to the standard [39], is the same as the intermediate state between the complete absence of scratching and complete scratching. The estimated amount of deformation α in the generalized notation is determined by the following relationship:

$$\alpha = \zeta\alpha_{II} + (1 - \zeta)\alpha_{I}, \tag{1}$$

where α defines the parameter of the considered deformation (deflection), α_I and α_{II} are the deformation parameters for the 1st and 2nd phase of the cross-section operation, respectively, while ζ is the distribution coefficient that takes into account the tensile stiffness. Factor ζ takes values according to the following relationship:

$$\zeta = \begin{cases} 0, & \text{for phase I (non-cracked cross-section),} \\ 1 - \beta\left(\dfrac{M_{cr}}{M_{Ek}}\right)^2, & \text{or phase II (cracked cross-section),} \end{cases} \tag{2}$$

where M_{cr} is the value of the critical moment (moment causing the first crack), while M_{Ek} is the characteristic value of the actual moment occurring in the bending element. While β is the coefficient determining the time of impact and influence of loads, including repetitive loads, on the amount of average deformation. The β coefficient in equation (2) takes the value $\beta = 1.0$ for a single short-term load and $\beta = 0.5$ for a long-term load and a multiple-repetitive load, respectively. The estimated deflection curvature $k_{cs.u}$ (in a cracked state) and $k_{cs.r}$ (in a non-cracked state) due to concrete contraction are described by the following relationships:

$$\begin{aligned} k_{cs.u} &= \frac{1}{r_{cs.u}} = \varepsilon_{cs}\alpha_e\frac{S_s}{I_{cu}}, \\ k_{cs.r} &= \frac{1}{r_{cs.r}} = \varepsilon_{cs}\alpha_e\frac{S_s}{I_{cr}}, \quad \alpha_e = \frac{E_s}{E_c}, \end{aligned} \tag{3}$$

where r_{cs} is the radius of the deflection curvature, ε_{cs} is the free contraction deformation, E_s and E_c, respectively, are the modulus of elasticity of the reinforcing steel and the modulus of concrete elasticity (without taking into account the phenomenon of creep), S_s is the static moment of the surface of the tensile reinforcement calculated with respect to the center of gravity of the entire section of the RC element, I_{cu} and I_{cr} are the moment of inertia of the entire RC section, respectively, in the non-cracked state and in the cracked state. Geometric quantities I_{cu}, I_{cr}, and S_s should be determined twice separately for the two considered phases.

The curvature of the bending element as a result of its own weight and external loads, separately in the non-cracked k_{cu} and cracked k_{cr} states, is expressed by the following relations:

$$k_{cu} = \frac{1}{r_{cu}} = \frac{M_{Ek}}{E_c I_{cu}}, \qquad k_{cr} = \frac{1}{r_{cr}} = \frac{M_{Ek}}{E_c I_{cr}}, \tag{4}$$

where k_{cu} is the curvature of r_{cu} radius (phase I – non-cracked state), while k_{cr} is the curvature of r_{cr} radius (phase II – cracked state).

The sum of the curvatures due to shrinkage and external loads together with the own weight will correspond to the total curvature, which can be considered separately for the stage before and after cracking.

$$\begin{aligned} k_c &= k_{cu} + k_{cs.u}, \quad \text{for phase I (non-cracked cross-section)}, \\ k_r &= k_{cr} + k_{cs.r}, \quad \text{for phase II (cracked cross-section)}, \end{aligned} \tag{5}$$

The final value of the curvature k should be interpolated between the extreme values – determined for phase I and II, according to the relationship (1). After taking into account the dependencies (3)–(5), equation (1) describes the deflection of the element in accordance with the requirements of the standard [39] as follows:

$$f_s = k_1 l_{eff}^2 [\zeta k_r + (1 - \zeta) k_u], \tag{6}$$

where f_s is the total deflection of the element taking into account its own weight, external loads, and contraction, k_1 is the coefficient taking into account the method of supporting the analyzed structure, and l_{eff} is the effective length of the considered element according to a previous study [39].

At the time of the occurrence of corrosion processes, the total deflection of the RC element f will be equal to the sum of deflections from static loads and contraction f_s as well as deflections caused by the reduction in the reinforcement cross-section on account of weight loss Δm due to the progressive electrode processes Δf_{corr} at time t.

$$f = f_s + \Delta f_{corr}. \tag{7}$$

The deflection of the RC element can be directly related to the corrosion current density i_{corr}, which is a function of the parameters describing the influence of the external environment, such as temperature, humidity, and concentration of chloride ions in accordance with analytical analysis [40,41].

$$i_{corr} = \frac{I_{corr}}{A_b} = 0.0092 \exp\left(8.37 + 0.618 \ln(1.69 C_{fc}) - \frac{3{,}034}{T} - 0.000105 R_{c,res} + A_1 t^{-0.215}\right), \tag{8}$$

where A_b is the surface of the rod on which the electrochemical processes take place in the considered time t, C_{fc} is the concentration of chloride ions, T is the temperature, A_1 is the coefficient experimentally determined to be 2.32 according to the report by Liu [40] or $A_1 = 2.35$ according to the report by Balafas and Burgoyne [41]. The concentration of chloride ions C_{fc} included in equation (8), apart from the depassivation of the reinforcement and the initiation of electrode processes, can be equated with the increase in the electrical conductivity of the porous liquid in the concrete. The influence of humidity H is included in the concrete resistance $R_{c,res}$ described by the following relationship [41]:

$$R_{c,res} = 90.537 H^{-7.2548} [1 + \exp(5 - 50(1 - H))], \tag{9}$$

where H is the humidity of the area under corrosion. According to Faraday's law, the theoretical weight loss of reinforcement Δm assuming an effective electrochemical equivalent of reinforcing steel k_{eff} [10], can be presented in the following form:

$$\Delta m = \int_0^t k_{eff} i_{corr} A_b \, dt, \tag{10}$$

where Δm is the weight loss of the reinforcement, and k_{eff} is the average value of the electrochemical equivalent of the reinforcing steel. Assuming that the reinforcement corrosion is uniformly distributed in the area of the analyzed reinforcement, and the loss of their mass is the same on the side surface of the bars, the change in the reinforcement diameter can be determined as follows:

$$\rho_{Fe} = \frac{\Delta m}{\Delta V} = \frac{\Delta m}{\frac{\pi \Delta \phi_d^2}{4} l_{eff}}, \quad \Delta \phi_d = \sqrt{\frac{4 \Delta m}{\rho_{Fe} l_{eff} \pi}}, \tag{11}$$

where ΔV is the volume of the analyzed reinforcement, l_{eff} is the beams in the axes of supports equal to the length of the reinforcement inserts, and $\Delta \phi_d$ is the diameter loss of a single reinforcing bar. Increments in the curvature of the element Δk_{cu} and Δk_{cr} after taking into account the loss of bar mass Δm progressing over time due to the development of corrosion processes at time t according to equation (10) will take the following form:

$$\Delta k_{cu} = \Delta \frac{1}{r_u} = \frac{M_{Ek}}{E_c I_{cu}(t)}; \quad \Delta k_{cr} = \Delta \frac{1}{r_r} = \frac{M_{Ek}}{E_c I_{cr}(t)}. \tag{12}$$

The above equations cover the situation in which the initiation of the corrosion process takes place before the cracking of the RC element (stage I of the structure's operation). By building the inverse equations, one can derive a relationship describing the corrosion current density as a function of total deflection, which is particularly important in the diagnosis of RC structures.

$$i_{corr} = \Delta t \left(\frac{M_{Ek}}{\Delta k_u E_{c,eff}(t) y^2} + \frac{M_{Ek}}{\Delta k_r E_{c,eff}(t) y^2} \right) \frac{\rho_{Fe} l_{eff}}{k_{eff} A_b}, \tag{13}$$

where I_{cr} is the moment of inertia of the cracked section, and y is the distance of the center of gravity of the section from the extreme tension fibers.

3 Analysis of deflection

3.1 Analytical analysis

For the analysis, a theoretical simply supported beam with the dimensions of the cross-section 250 mm × 500 mm and the length in the axes of the supports equal to l_{eff} = 4,000 mm, made of C30/37 class concrete was adopted (Figure 1). It was assumed that the beam would be loaded with a concentrated force with the characteristic value P = 120 kN in the middle of the span, thus generating a characteristic bending moment equal to M_{Ek} = 120 kNm. Tensile reinforcement of a beam was adopted from 5 bars with a diameter of ϕ_{d} = 16 mm. The top (compression) and transverse reinforcement in the form of stirrups were omitted for theoretical calculations. It was assumed that the concrete cover was equal to c_{nom} = 40 mm, which defined the center of gravity of the tensile reinforcement at a distance a_1 = 48 mm from the lower edge of the beam (bars arranged in one row) (Figure 1).

Influence of corrosion of reinforcing steel was taken into account using the actual results of measuring the current intensity during the so-called accelerated corrosion test performed within the framework of the study [10]. The average value of changes in current intensity I_{corr}, obtained from four analyzed samples, for which measurements were made, was used for the calculations. This value was rescaled in the proportion of the side surface of the reinforcement, on which the possible course of the electrode processes was assumed (scale factor k_{s} = 160). Eventually, the history of changes in the current intensity during the experiment took the form presented in the graphs (Figure 2). Then, according to Faraday's law, the theoretical weight loss of the reinforcement was calculated (Figure 2a) assuming the effective electrochemical equivalent of reinforcing steel k_{eff} = 0.006271 g/(μA · year) according to the report by Krykowski et al. [10] in accordance with the relationship (10). Then, assuming the steel density to be equal to the iron density ρ_{Fe} = 7,850 kg/m^3, the course of changes in the loss of the tension reinforcement surface area was determined in accordance with equation (11) (Figure 2b).

Deflection calculations were performed assuming the same amount of bending moment over time t = 622 h, which corresponded to the time interval of the analysis of experimental samples under the accelerated corrosion test described by Krykowski et al. [10]. The changes in the diameter of reinforcing bars calculated according to equation (12) were related to the change in the deflection value of the analyzed beam (equation (9)) without taking into account the creep effect. Due to the very short analysis time, it was assumed that the influence of creep is negligible. The list of parameters of concrete and reinforcing steel adopted for the calculations is presented in Table 1.

3.2 Numerical analysis

FEM analysis was performed using the GID-Atena system. Using the symmetry of the test element, only half of the beam was modeled in order to reduce the number of finite elements and nodes. The whole beam was discretized with 105 linear finite elements and 92 hexagonal solid elements, generating 920 nodes. The test element was articulated and then loaded with a force of 120 kN in the middle of the theoretical span in accordance with the assumptions made for the analytical calculations (Figure 3a). Steel elements measuring 100 mm × 250 mm and 50 mm thick were modeled at the fulcrum and load was applied to increase the pressure zone and uniform stress distribution.

The loss of reinforcement mass in the considered time period due to corrosion processes was simulated by a change in the diameter of the reinforcing bars (equation (11)) in the next 10 calculation steps. The course of

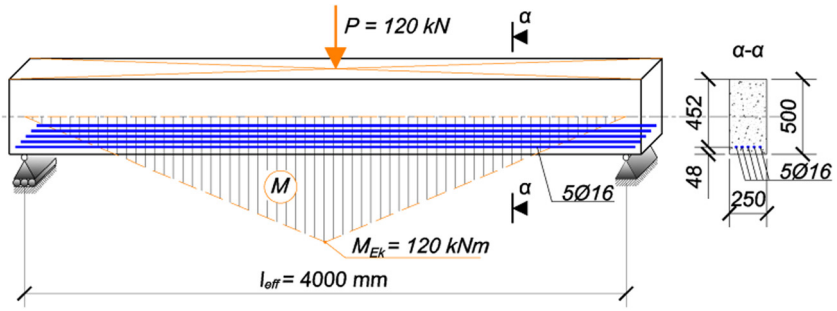

Figure 1: Diagram of the theoretical beam accepted for analysis.

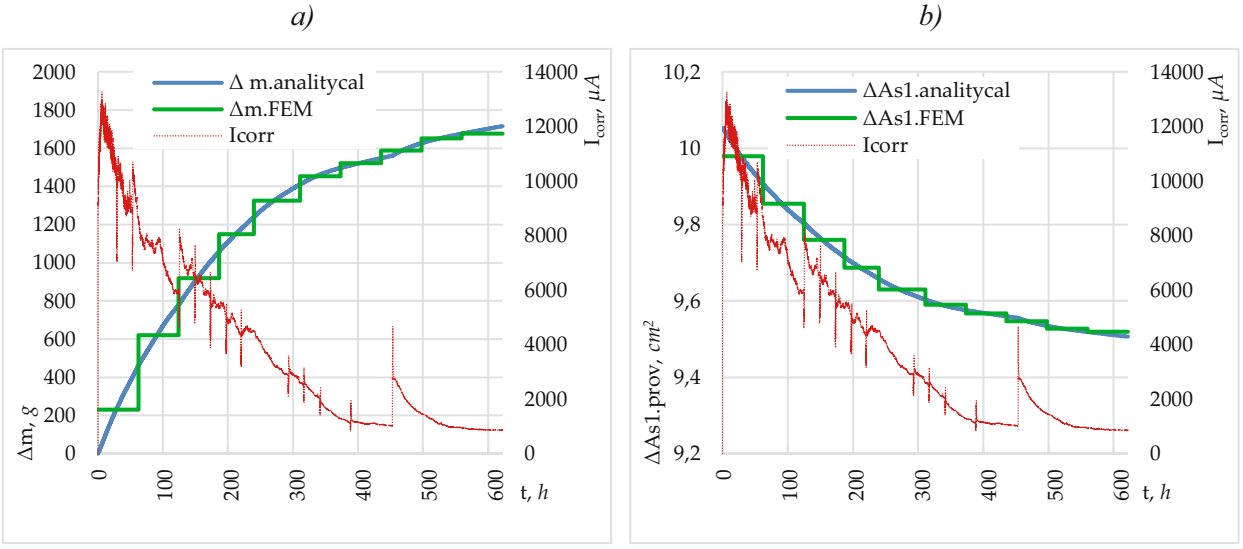

Figure 2: The course of changes as a function of the corrosion current I_{corr}: (a) weight loss of the analyzed beam reinforcement and (b) loss of the analyzed reinforcement area.

Table 1: Material characteristics of concrete and reinforcing steel adopted for analytical calculations

Concrete C30/37	
Young's modulus, E (GPa)	32
Poisson's ratio, ν (1)	0.2
Medium tensile strength, f_{ctm} (MPa)	2.9
Reinforcing steel B500SP	
Young's modulus, E (GPa)	200
Poisson's ratio, ν (1)	0.3
Characteristic yield point of steel, f_{yk} (MPa)	500

changes in the cross-sectional area of the reinforcement due to the progressing corrosion process is presented in the diagram (Figure 2b), including the analytically calculated reduction in the cross-sectional area of the reinforcement. The sum of the mass of the elevated iron ions in the next 10 calculation steps was the total weight loss of the reinforcement determined according to equation (10) after the theoretical time t = 622 h. The computer analysis was performed using the elastic-plastic-brittle concrete model CC3DNonLinCementitious2 applied in the GID-Atena calculation system. In terms of tensile stresses, the Rankine criterion was used, while in other cases, the Menetrey-William model was used. The mechanical parameters of the concrete were determined in accordance with the software manual for concrete class C30/37. In order to stabilize the results and improve the convergence of the calculations, the possibility of aggregate interlock, shear factor, and the parameter including tension stiffening were adopted. Reinforcement bars were defined as linear elements with the CCReinforcement model in the system (elastic-plastic without reinforcement). The auxiliary steel elements were

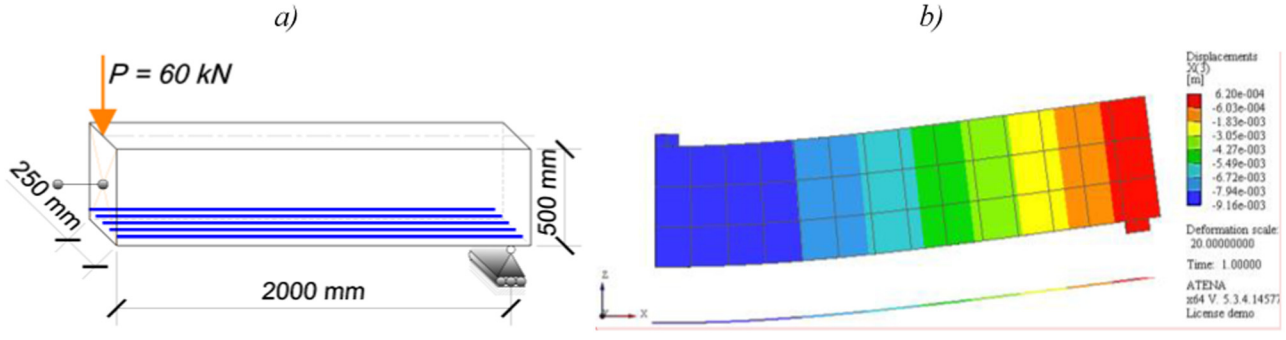

Figure 3: Beam accepted for numerical analysis: (a) static diagram and (b) the result of the numerical analysis in the form of a map of the beam deflection changes.

modeled using the Huber-Mises-Hencky elastic-plastic material (CC3D Bilinear steel Von Mises). The material parameters adopted for the FEM analysis are summarized in Table 2.

4 Results

As a result of the numerical analysis, the course of changes in the deflection of the RC element during the progressive corrosion of the reinforcement was obtained, which was compared with the results of analytical calculations (Figure 4).

In the initial stage (immediately before the theoretical development of corrosion processes), only due to external loads and shrinkage, the deflection calculated by the analytical method was $f_{0.\text{analitycal}} = 8.86$ mm. After the theoretical time of 622 h of the accelerated corrosion test, the deflection of the RC element was calculated, which resulted in $f_{1.\text{analitycal}} = 9.14$ mm. Therefore, the difference in the beam deflection resulting solely from the progress of corrosion processes was equal to $\Delta f_{\text{analitycal}} = 0.28$ mm. The initial deflection of the beam, determined based on the numerical analysis, was $f_{0.\text{FEM}} = 8.87$ mm, while after exceeding the theoretical duration of the corrosion process $f_{1.\text{FEM}} = 9.13$ mm. Thus, the numerical analysis showed the difference in beam deflections equal to $\Delta f_{\text{FEM}} = 0.26$ mm. The obtained

Table 2: Material characteristics of concrete and steel adopted for the FEM analysis

Concrete C30/37	
Young's modulus, E (GPa)	32
Poisson's ratio, ν (1)	0.2
Medium tensile strength, f_{ctm} (MPa)	2.9
Fracture energy, G_{f} (kN/m)	0.0422
Minimum crack spacing, a_{crack} (mm)	200
Maximum size of the aggregate, d_{agg} (mm)	16
Shear factor, (1)	20
Tension stiffening, (1)	1
Reinforcing steel B500SP	
Young's modulus, E (GPa)	200
Poisson's ratio, ν (1)	0.3
Characteristic yield point of steel, f_{yk} (MPa)	500
Hardening modulus, H_{M} (GPa)	10
Steel S235 (support elements)	
Young's modulus, E (GPa)	200
Poisson's ratio, ν (1)	0.3
Characteristic yield point of steel, f_{yk} (MPa)	500

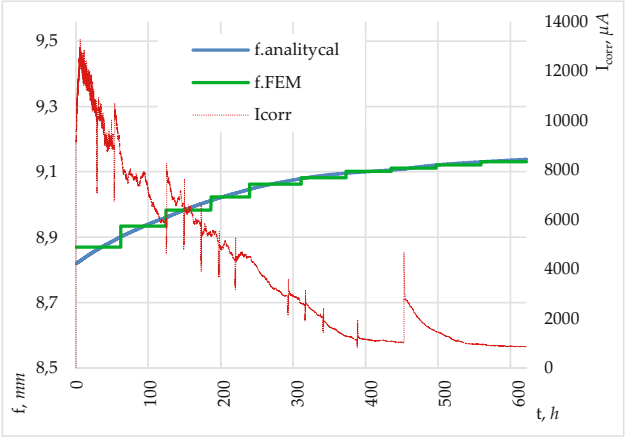

Figure 4: The course of changes in beam deflection under the influence of corrosion of reinforcing steel.

results of the calculations were the basis for the determination of the current I_{corr} and the current density i_{corr}, which were determined in two approaches. In the first, on the basis of the results of analytical calculations, and in the second, on the basis of the results of numerical analysis with the use of FEM. In the first stage, on the basis of the history of the deflection changes in time, the curvature of the element was determined, and then, in accordance with equation (13), the course of changes in the current intensity and its intensity density were determined. In the second approach, the results of numerical analyzes were the basis for determining the desired quantities. The results of the analysis are summarized in the form of the evolution of the changes in the current intensity I_{corr} (Figure 5a) and the current density i_{corr} (Figure 5b) during the accelerated corrosion test according to Krykowski et al. [10].

5 Discussion

The obtained results of the estimated value of the corrosion current I_{corr} and the current density i_{corr} in the analytical approach fully coincide with the history of changes in these values, which are the starting point for the calculation of deflections according to the rescaled value in accordance with the work [10]. This proves the correctness of the calculations made and the possibility of using inverse equations to determine the corrosion current and the current density. The beam deflection simulations with the use of FEM confirmed the correctness of the calculated deflections in the analytical method. The applied division of the course of changes

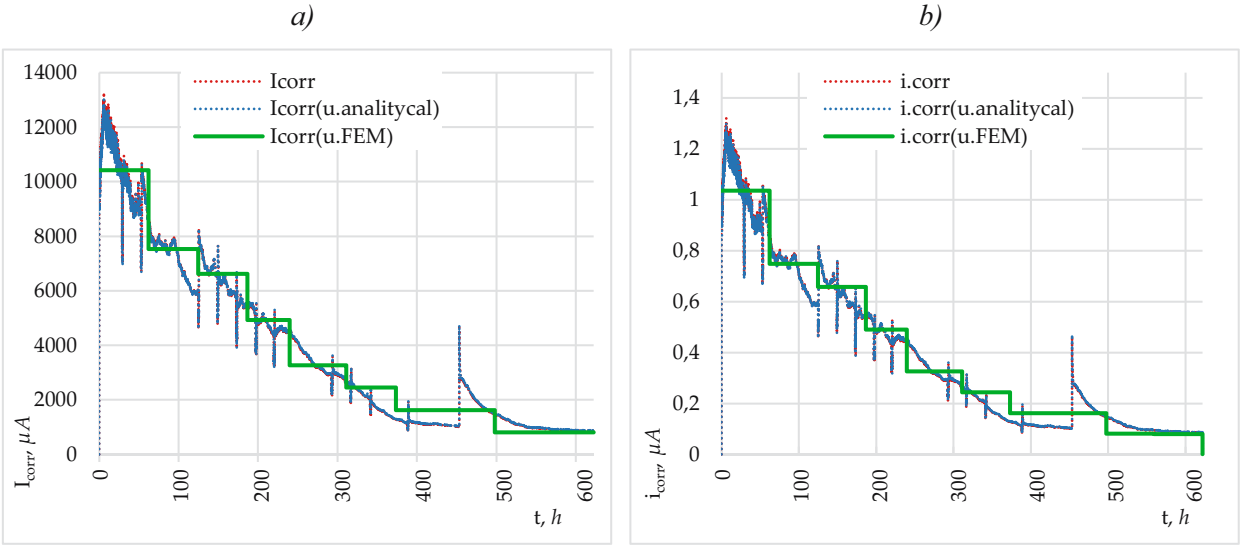

Figure 5: Estimated history of: (a) current I_{corr} and (b) current density i_{corr}.

in the intensity of the corrosion current can be equated with the cyclical manual measurement of the deflection of the RC element in *in situ* conditions. The interval estimated evolution of changes in the corrosion current intensity and current density very well reflects the actual parameters occurring in the element. The accuracy of the results is determined by the number of intervals determined by the frequency of real deflection measurements. Although the most accurate would be the continuous measurement of deflection, the proposed method shows satisfactory results for cyclic measurements. The essence of the presented approach is to maintain a very high degree of diligence in measuring the deflection of the actual structure and to determine the external loads and shrinkage, for which there is an initial deflection without the influence of reinforcement corrosion. The differences between the deflection in the state before the corrosion processes initiate and the deflection in the corroded state of the reinforcement are small. However, remembering what the corrosion process affects, i.e. not only the loss of the bar mass, and thus a decrease in the amount of reinforcement in the element, but also a change in the yield strength of the reinforcing steel and a change in the adhesion forces at the contact between steel and concrete the actually expects greater differences in the analyzed deflections. These aspects were not taken into account at this stage, but it was planned during the development and improvement of the proposed method. The second issue that was planned to be taken into account at the stage of development of the proposed method is the analysis of the uneven distribution of areas within which corrosion processes take place and the discrepancies in their intensity. The proposed method may be the first stage in the diagnosis of possible corrosion processes and constitute the basis for taking further steps in advanced structure diagnostics. The presented method is based solely on the theoretical analysis of analytically calculated deflections and then verified with the use of FEM, which makes it fully theoretical. At a later stage, it is necessary to undertake an experimental verification of the proposed method on the basis of full-size test elements in laboratory conditions (beams, plates) and measurements of the actual structure deflections. A separate research problem related to the deflection of RC elements are the changes in the Young's modulus of the reinforcing steel subject to corrosion processes and the adhesion forces at the interface between steel and concrete, the results of which are also planned to be included in the further development of the proposed method.

6 Conclusion

- The article presents an attempt to apply the analysis of deflection of RC elements in order to initially estimate the value of the corrosion current I_{corr} and the current density i_{corr}, which is a new, original element of analysis not previously undertaken in the research environment of the subject. The presented results of the analytical and numerical calculations provide the basis for the following conclusions.
- The presented method reflects the real electrical parameters of the corrosion process very well. This is confirmed by the

verification of the calculation obtained with the use of inverse equations based on the deflection curvature of the test element and described in Section 2 of this article of the evolution of changes in the intensity of the corrosion current I_{corr} based on the initially assumed course of changes of this value. The performed calculations show that it is possible to estimate the corrosion current density on the basis of the deflection of RC elements affected by environmental aggression.

- The application of the FEM analysis allowed in the first stage to verify the calculated deflections with the analytical method. Second, the interval assumption of the weight loss of the reinforcement reflected the cyclic measurements of the deflection of the RC element in finite time intervals. The results presented in the charts (Figure 5) indicate the possibility of using cyclic deflection measurements to estimate the parameters sought with a satisfactory result, which are burdened with small errors resulting directly from the assumption of cyclical deflection measurements of the analyzed beam.
- The presented analysis is theoretical with the use of analytical calculations, subsequently confirmed by a numerical method. It should be verified on the basis of test elements in laboratory conditions and measurements of the deflections of the existing structures. An additional element subject to further research is the extension of the proposed methodology with aspects related to the possible change in the Young's modulus of the reinforcing steel, changes in the adhesion at the interface between steel and concrete, or differentiation and taking into account the uneven distribution of areas affected by corrosion processes.

Conflict of interest: Author states no conflict of interest.

References

[1] Koniorczyk M, Gawin D. Numerical modelling of coupled heat, moisture and salt transport in porous materials. Comput Assist Mech Eng Sci. 2006;13(1):565–74.

[2] Martín-Pérez B. Service life modelling of R.C. Highway structures exposed to chlorides. PhD thesis. Canada: University of Toronto; 1999.

[3] Černý R, Rovnaníková P. Transport Processes in Concrete. London; New York: CRC Press; 2002. p. 275–332.

[4] Ožbolt J, Balabanić G, Periškić G, Kušter M. Modelling the effect of damage on transport processes in concrete. Constr Build Mater. 2010;24(9):1638–48.

[5] Saetta A, Scotta R, Vitaliani R. Mechanical behavior of concrete under physical-chemical attacks. J Eng Mech. 1998;124(10):1100–9.

[6] Xi Y, Bazant ZP. Modeling chloride penetration in saturated concrete. J Mater Civ Eng. 1999;11(1):58–65.

[7] Sola E, Ožbolt J, Balabanić G, Mir ZM. Experimental and numerical study of accelerated corrosion of steel reinforcement in concrete: Transport of corrosion products. Cem Concr Res. 2019;120(7):119–31.

[8] Michel A, Pease BJ, Peterová A, Geiker MR, Stang H, Thybo AEA. Penetration of corrosion products and corrosion-induced cracking in reinforced cementitious materials: Experimental investigations and numerical simulations. Cem Concr Compos. 2014 Mar;47:75–86.

[9] Suwito C, Xi Y. The effect of chloride-induced steel corrosion on service life of reinforced concrete structures. Struct Infrastruct Eng. 2008;4(3):177–92.

[10] Krykowski T, Jaśniok T, Recha F, Karolak M. A cracking model for reinforced concrete cover, taking account of the accumulation of corrosion products in the ITZ layer, and including computational and experimental verification. Materials. 2020;13(23):1–17.

[11] Maaddawy TE, Soudki K. A model for prediction of time from corrosion initiation to corrosion cracking. Cem Concr Compos. 2007;29(3):168–75.

[12] Almusallam AA. Effect of degree of corrosion on the properties of reinforcing steel bars. Constr Build Mater. 2001;15(8):361–8.

[13] Apostolopoulos CA, Papadopoulos MP, Pantelakis SG. Tensile behavior of corroded reinforcing steel bars BSt 500s. Constr Build Mater. 2006;20(9):782–9.

[14] Fischer C. Auswirkungen der Bewehrungskorrosion auf den Verbund zwischen Stahl und Beton. Stuttgart, Germany: Institut für Werkstoffe im Bauwesen der Universität Stuttgart; 2012.

[15] Capozucca R. Damage to reinforced concrete due to reinforcement corrosion. Constr Build Mater. 1995;9(5):295–303.

[16] German M, Pamin J. FEM simulations of cracking in RC beams due to corrosion progress. Arch Civ Mech Eng. 2015;15(4):1160–72.

[17] Alami EE, Fekak F, Garibaldi L, Moustabchir H, Elkhalfi A, Scutaru ML, et al. Numerical study of the bond strength evolution of corroded reinforcement in concrete in pull-out tests. Appl Sci. 2022;12:654.

[18] Altoubat S, Maalej M, Shaikh FUA. Laboratory simulation of corrosion damage in reinforced concrete. Int J Concr Struct Mater. 2016;10(3):383–91.

[19] Sæther I, Sand B. FEM simulations of reinforced concrete beams attacked by corrosion. Nordic Concr Res. 2009;39:15–32.

[20] Castel A, Franfois R, Arliguie G. Mechanical behaviour of corroded reinforced concrete beams - Part 1: Experimental study of corroded beams. Mater Struct. 2000;33:539–44.

[21] Recha F, Krykowski T, Jaśniok T. Numeryczna symulacja spadku nośności konstrukcji żelbetowej w wyniku korozji zbrojenia. Proceedings of the 15th International Conference on New Trends in Statics and Dynamics of Buildings. Bratislava: Bratislava, Slovakia Faculty of Civil Engineering STU Bratislava Slovak Society of Mechanics SAS Tecnológico de Monterrey, Campus Puebl; 2017.

[22] Shen J, Gao X, Li B, Du K, Jin R, Chen W, et al. Damage evolution of RC beams under simultaneous reinforcement corrosion and sustained load. Materials. 2019;12(4):1–16.

[23] Wang Z, Jin W, Dong Y, Frangopol DM. Hierarchical life-cycle design of reinforced concrete structures incorporating durability, economic efficiency and green objectives. Eng Struct. 2018 Feb;157:119–31.
[24] Li L, Mahmoodian M, Khaloo A, Sun Z. Risk-cost optimized maintenance strategy for steel bridge subjected to deterioration. Sustainability. 2022;14(1):436.
[25] Recha F, Nagel P. Principles of conducting periodic technical tests of building objects in the field in safety and use. Builder. 2022;295(2):12–4.
[26] Van Steen C, Verstrynge E. Degradation monitoring in reinforced concrete with 3D localization of rebar corrosion and related concrete cracking. Appl Sci. 2021;11(15):6772.
[27] Raczkiewicz W, Wójcicki A. Temperature impact on the assessment of reinforcement corrosion risk in concrete by galvanostatic pulse method. Appl Sci (Switz). 2020;10(3):13–5.
[28] Zybura A, Jaśniok M, Jaśniok T. Diagnostyka konstrukcji żelbetowych. Badania korozji zbrojenia i właściwości ochronnych betonu, t.2. Warszawa: Wydawnictwo Naukowe PWN; 2011.
[29] Recha F. Modeling the degradation of reinforced concrete elements as a result of reinforcement corrosion. PhD thesis. Gliwice, Poland: Silesian University of Technology; 2021.
[30] Grandić D, Bjegović D, Grandić IŠ. Deflection of reinforced concrete beams simultaneously subjected to sustained load and reinforcement corrosion. Structural Engineers World Congress; 2011.
[31] Negrutiu C, Sosa IP, Constantinescu H, Heghes B. Crack Analysis of Reinforced High Strength Concrete Elements in Simulated Aggressive Environments. Procedia. Technology. 2016;22:4–12.
[32] Recha F. Method for estimating corrosive current based on deflection of reinforced concrete elements - theoretical approach. Sci Noteb Katow Sch Technol Chapter Civ Eng Transp. 2022;14:57–64.
[33] Wanyou Z, Ruiyuan Z, Lijuan X. Corrosion of reinforced concrete in accelerated tests. Adv Mater Res. 2013;610–613(3):485–9.
[34] Loukil O, Adelaide L, Bouteiller V, Quiertant M, Ragueneau F, Bourbon X, et al. Experimental study of corrosion-induced degradation of reinforced concrete elements. International RILEM Conference on Materials, Systems and Structures in Civil Engineering Conference Segment on Service life of cement-Based Materials and Structures. Lyngby, Denmark: Technical University of Denmark; 2017.
[35] Bhalgamiya S, Tivadi G, Jethva M. Techniques for Accelerated Corrosion Test of Steel Concrete for Determining Durability. Int Res J Eng Technol. 2018;5(4):4399–402.
[36] Deb S. Accelerated short-term techniques to evaluate corrosion in reinforced concrete structures. Masterbuilder. 2012:248–55.
[37] Arredondo-Rea SP, Corral-Higuera R, Gómez-Soberón JM, Gámez-García DC, Bernal-Camacho JM, Rosas-Casarez CA, et al. Durability parameters of reinforced recycled aggregate concrete: Case study. Appl Sci. 2019;9(4):617.
[38] Vidal T, Castel A, François R. Analyzing crack width to predict corrosion in reinforced concrete. Cem Concr Res. 2004;34(1):165–74.
[39] Polish Committee of Normalization. Norm PN-EN 1992-1-1 Eurocode 2: Design of concrete structures. Part 1-1: General rules and regulations for buildings; Warsaw; 2008.
[40] Liu Y. Modeling the time to corrosion cracking of the cover concrete in chloride contaminated reinforced concrete structures. PhD thesis. Blacksburg, Virginia, USA: Virginia Polytechnic Institute and State University; 1996.
[41] Balafas I, Burgoyne CJ. Environmental effects on cover cracking due to corrosion. Cem Concr Res. 2010;40(9):1429–40.